JACS
JOURNAL OF THE AMERICAN CHEMICAL SOCIETY

COMMUNICATION

pubs.acs.org/JACS

Wet-Chemistry-Assisted Nanotube-Substitution Reaction for High-Efficiency and Bulk-Quantity Synthesis of Boron- and Nitrogen-Codoped Single-Walled Carbon Nanotubes

Xiaoxia Yang,[†] Lei Liu,[†] Muhong Wu,[†] Wenlong Wang,[*,†] Xuedong Bai,[*,†] and Enge Wang[*,‡]

[†]Beijing National Laboratory for Condensed Matter Physics, Institute of Physics, Chinese Academy of Sciences, Beijing 100190, China
[‡]International Center for Quantum Materials, School of Physics, Peking University, Beijing 100871, China

Supporting Information

ABSTRACT: We present an innovative wet-chemistry-assisted nanotube-substitution reaction approach for the highly efficient synthesis of boron- and nitrogen-codoped single-walled carbon nanotubes ($B_xC_yN_z$-SWNTs) in bulk quantities. The as-synthesized ternary system $B_xC_yN_z$-SWNTs are of high purity and quality and have fairly homogeneous B and N dopant concentrations. Electrical transport measurements on SWNT-network thin-film transistors revealed that the $B_xC_yN_z$-SWNTs were composed primarily of the semiconducting nanotubes, in contrast to the starting pristine C-SWNTs, which consisted of a heterogeneous mixture of both semiconducting and metallic types.

Substitutional doping of carbon nanotubes (C-NTs) with boron and/or nitrogen to tune their electronic properties is of fundamental and practical importance.[1,2] In the periodic table, B and N are the nearest neighbors of C, and simultaneous B/N codoping of C-NTs through partial substitution of the C−C units in the tube-shell lattice with isoelectronic B−N units was expected to give rise to the ternary system $B_xC_yN_z$-NTs, which, with stoichiometry variations, should exhibit tunable semiconducting properties intermediate between those of metallic or small-gap C-NTs and insulating BN-NTs.[2,3] In comparison with pristine C-NTs that naturally consist of two-thirds semiconducting and one-third metallic nanotubes, the intrinsic semiconducting nature of the ternary $B_xC_yN_z$-NTs would make them more amenable to nanotube-based electronics and optoelectronics, sensors, and other applications.[1−3] However, to date, research on $B_xC_yN_z$-NTs has been severely hindered by the challenging difficulties involved in their synthesis, especially the synthesis of single-walled nanotubes (SWNTs), despite the recent advances by us[3] and others.[4]

Generally speaking, there are two different strategies for producing the ternary $B_xC_yN_z$-NTs: the direct growth route [by means of, e.g., chemical vapor deposition (CVD), arc discharge, and laser ablation] and the postsynthetic nanotube-substitution reaction route.[1b−d] Specifically, the latter approach refers to the use of the presynthesized C-NTs as a starting precursor that undergoes a carbothermal reaction with B_2O_3 vapor at elevated temperature (1200−1700 °C) under a N_2 or NH_3 atmosphere, through which the B and N heteroatoms are incorporated into the honeycomb tube-shell lattice of the C-NTs, thereby resulting in the formation of the ternary $B_xC_yN_z$-NTs or

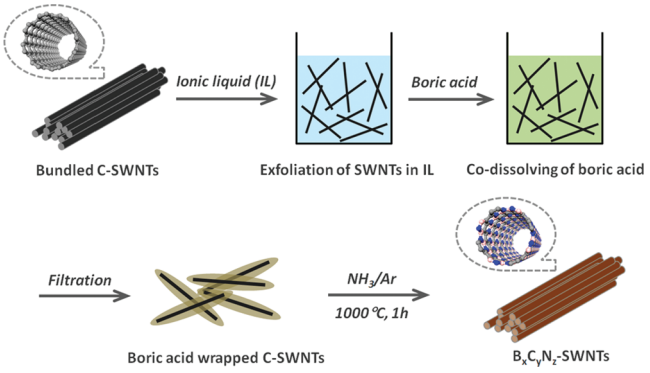

Figure 1. Schematic illustration of the wet-chemistry-assisted nanotube-substitution reaction process for $B_xC_yN_z$-SWNT synthesis, which involves exfoliation of the bundled C-SWNTs in an IL, wrapping of the exfoliated SWNTs with boric acid, and carbothermal substitution reaction at elevated temperature.

even pure BN-NTs.[1c,d,5] This nanotube-substitution reaction approach was first pioneered by Han et al.[5] and later further developed by Golberg and co-workers.[6] By employing *multiwalled* C-NTs as the precursor for substitution, they demonstrated the successful synthesis of *multiwalled* BN- and $B_xC_yN_z$-NTs in bulk-quantities.[5−7] Unfortunately, however, this nanotube-substitution reaction approach was found to be far less effective when applied to B/N codoping of *SWNTs*.[8] The prime reason lies in the bundling phenomena of the starting C-SWNTs. As a result of the extraordinary cohesive interaction between neighboring nanotubes, SWNTs have a strong tendency to spontaneously form densely bundled ropes in their native state.[9] When the bundled C-SWNTs are subjected to the carbothermal substitution reaction process, only the small fraction of SWNTs localized at the outermost fragments of the bundles are chemically accessible to the gaseous B and N reactants, whereas the inner SWNTs are protected from the treatment by the outer ones.[6,8]

Herein we report on an innovative wet-chemistry-assisted nanotube-substitution reaction approach (Figure 1) for the highly efficient synthesis of ternary $B_xC_yN_z$-SWNTs in bulk quantities. An initial and key step of this approach was exfoliation and dispersion of the starting C-SWNTs (HiPCO, superpurified) in a

Received: March 11, 2011
Published: August 02, 2011

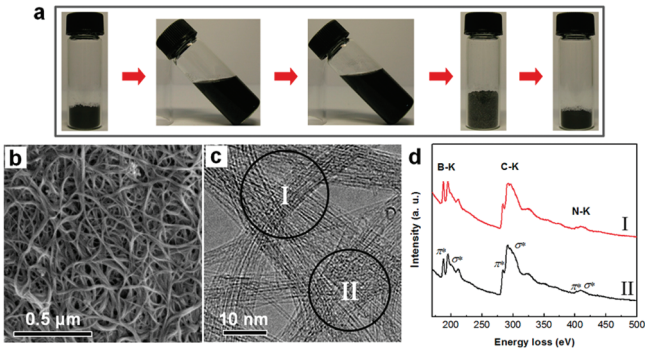

Figure 2. (a) Photographs showing the processing of SWNTs in a sequence corresponding to Figure 1. The starting HiPCO C-SWNTs, the suspension of exfoliated SWNTs in $BMIBF_4$, the suspension after mixing with boric acid, the boric acid-wrapped SWNTs, and the resultant $B_xC_yN_z$-SWNTs after the carbothermal substitution reaction at 1000 °C are shown left to right. (b, c) Typical (b) SEM and (c) TEM images of the as-synthesized $B_xC_yN_z$-SWNTs. (d) Corresponding EELS spectra recorded at the two different probe positions marked in (c).

room-temperature ionic liquid (IL), 1-*n*-butyl-3-methylimidazolium tetrafluoroborate ($BMIBF_4$). It has recently been reported that the imidazolium-based room-temperature ILs are good solvents for large-scale processing of C-SWNTs, where the bundled SWNT ropes can be exfoliated and dispersed as individual nanotubes or very fine bundles with nanotube concentrations of up to 1 wt %.[10] Following the debundling and dispersing step, an appropriate amount of boric acid (H_3BO_3, which was later converted into B_2O_3 through dehydration at high temperature) was then codissolved into the C-SWNT suspension, where each of the exfoliated individual SWNTs would be equally exposed to the boric acid molecules. Next, the suspension was vacuum-filtered using a PTFE membrane (1 μm), and after removal of the residual $BMIBF_4$ by CH_2Cl_2 washing followed by vacuum drying, boric acid-wrapped C-SWNTs were obtained as a homogeneous gray powder. The boric acid-wrapped C-SWNTs were then subjected the carbothermal substitution reaction at an optimized temperature of 1000 °C with a supplied NH_3 gas flow. Experimental details of the synthetic process are presented in the Supporting Information (SI). Figure 2a shows optical photographs of the processing sequence for 100 mg of the starting C-SWNTs in a typical experimental run.

Representative scanning electron microscopy (SEM) and transmission electron microscopy (TEM) images of the as-synthesized bulk quantity of $B_xC_yN_z$-SWNTs are displayed in Figure 2b,c, respectively. As can be clearly seen, after the high-temperature carbothermal reaction, the resultant SWNTs are rebundled and form entangled SWNT ropes again. Importantly, the as-synthesized $B_xC_yN_z$-SWNTs are of high purity and quality rivaling that of the starting superpurified HiPCO C-SWNTs. Detailed TEM investigations revealed that the ternary $B_xC_yN_z$-SWNTs normally have straight and smooth tube-shell structures with a diameter distribution similar to that of the pristine C-SWNTs before the substitution reaction. Therefore, it is believed that the topological structures of the SWNTs remained nearly intact during the carbothermal substitution reaction accomplished at the optimized temperature of 1000 °C. However, this was no longer the case for a higher reaction temperature such as 1150 °C, as will be discussed shortly.

The elemental compositions of the as-synthesized $B_xC_yN_z$-SWNTs were carefully examined using electron energy loss

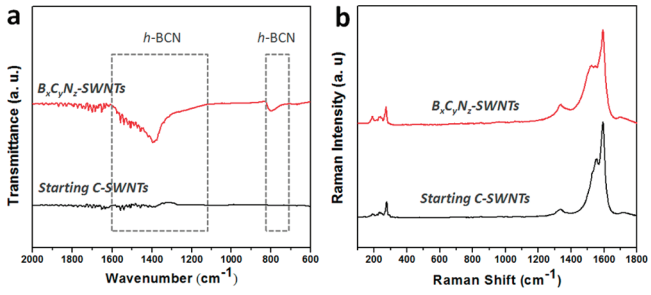

Figure 3. Typical (a) FT-IR and (b) Raman spectra of the starting C-SWNTs (black) and the doped $B_xC_yN_z$-SWNTs (red). The IR spectra are shown over the enlarged range of 600 to 2000 cm^{-1}.

spectroscopy (EELS). Figure 2d shows two EELS spectra probed at the two different positions marked in Figure 2c. Both spectra display the definite core-loss K-edges of B, C, and N located at 188, 284, and 401 eV, respectively. The well-defined features of the 1s $\rightarrow \pi^*$ and 1s $\rightarrow \sigma^*$ transitions are characteristic of the graphitic sp^2 bonding geometry of all the three elements, confirming that we achieved the true substitutional incorporation of B and N dopants into the SWNT lattice. Quantification of the two EELS spectra depicted in Figure 2d gave very close dopant concentrations of ~10 atom % for B and ~9 atom % for N. Importantly, nearly identical doping levels were also obtained for numerous EELS runs at different probe positions on the same batch of sample, indicating that the as-synthesized ternary $B_xC_yN_z$-SWNTs have fairly homogeneous elemental compositions.

Complementary evidence for the substitutional incorporation of B and N dopants into the tube-shell lattice of the C-SWNTs was also provided by X-ray photoelectron spectroscopy (XPS) characterization. As shown in Figure S4 in the SI), from the curve-fitted XPS spectra of B 1s, C 1s, and N 1s core-level electrons, the existence of sp^2-bonded B−C, B−N, and C−N bonding structures can be clearly identified, and the portions of B−C and C−N bonds rival that of the B−N bonds, suggesting that the constituent B, C, and N elements have a real ternary bonding nature within the tube-shell lattice.[1c,d,11] IR spectroscopy was also useful for obtaining qualitative insight about the formation of hexagonal $B_xC_yN_z$ (*h*-BCN) ternary phases.[11b,c,12] Figure 3a shows typical Fourier transform IR (FT-IR) spectra of SWNTs before and after B and N dopant incorporation. As can be seen, whereas the starting pristine C-SWNTs are essentially infrared-inactive (because graphitic C networks do not support a static dipole moment),[13] the IR spectrum of the doped $B_xC_yN_z$-SWNTs clearly shows the qualitative features characteristic of *h*-BCN.[11b,c,12] Specifically, the broad, strong IR absorption band over the range 1120−1600 cm^{-1} (with the main peak centered at 1392 cm^{-1}) corresponds to the in-plane stretching vibrations between atoms within the fused $B_xC_yN_z$ heterorings, and the minor absorption band at 710−830 cm^{-1} is ascribed to the corresponding out-of-plane bending modes (see Figure S1b for more details).[12] Apart from the IR results, the Raman spectrum of the $B_xC_yN_z$-SWNTs also shows distinct differences from that of the starting C-SWNTs, namely, much stronger disorder-induced D-band scattering and an appreciable line broadening for the tangential G band, as depicted in Figure 3b. These Raman features can be rationalized as a consequence of the substitutional doping of C-SWNTs with B and N heteroatoms, which leads to relaxation of the Raman selection rule for *K*-point phonons and a breakdown of the selection rule for zone-center phonon excitation.[14]

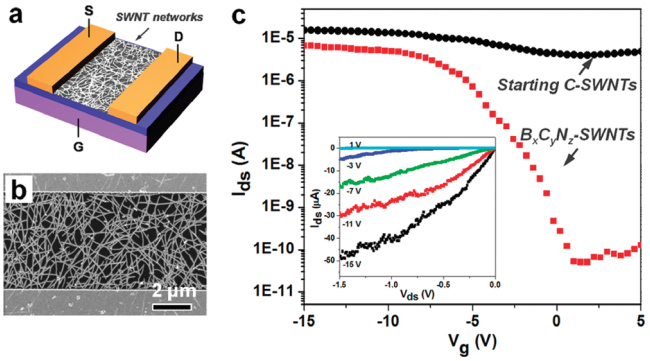

Figure 4. (a) Schematic illustration of the device geometry of an SWNT-network TFT with Ti/Au (2 nm/70 nm) source and drain contacts and SiO_2 (300 nm) as the gate dielectric. (b) SEM image of a typical device with a channel length of ~5 μm. (c) Representative room-temperature $I_{ds}-V_g$ transfer characteristics recorded at V_{ds} = 0.1 V for devices built from dense percolating networks of $B_xC_yN_z$-SWNTs (red) and the starting C-SWNTs (black). The inset shows $I_{ds}-V_{ds}$ output characteristics at various values of V_g for the $B_xC_yN_z$-SWNT device. To ensure a fair comparison of electronic analysis, the SWNT densities and device geometries were controlled to be nearly identical for these devices.

In our present study, the temperature of the substitution reaction is a crucial factor that sensitively affects the substitutional B/N doping process of C-SWNTs. As mentioned above, the optimized temperature was found to be ~1000 °C, and it turned out that a decrease in the reaction temperature to 900 °C resulted in minor or no doping of the starting C-SWNTs. On the other hand, when the temperature was increased to 1150 °C, the single-shell tube structure was found to deteriorate severely, causing the majority of the SWNTs to collapse and be transformed into highly defective but much more heavily doped thick $B_xC_yN_z$ nanofibers (see Figure S5). It is important to note that similar structural degradation behavior was also reported by Golberg and co-workers[6] in prior studies of carbothermal substitution reactions using bundled C-SWNT ropes as starting materials, but the corresponding processing temperature was much higher than in our case for the debundled SWNTs. In fact, in our study, we also conducted several control experiments employing bundled C-SWNTs as the precursor for the carbothermal substitution reaction, and neither SWNT deformation nor efficient B/N doping was observed to occur at the highest tested temperature of 1150 °C. These results suggest that the debundled C-SWNTs are much more susceptible to the substitution reaction than the bundled C-SWNT ropes and therefore highlights the key importance of the initial IL-based SWNT debundling step.

To determine whether B/N codoping successfully modified the electronic properties of the C-SWNTs and to demonstrate their applicability in nanoelectronic devices, we comparatively investigated the electrical transport properties of the SWNTs before and after B/N doping through fabrication of SWNT-network thin-film transistors (TFTs) (Figure 4a) according to a published procedure (see the SI for experimental details).[15b] As shown in Figure 4c, a dense percolating network of the starting C-SWNTs displayed the typical undepletable transfer characteristics with a low on/off ratio of ~5 due to the presence of both semiconducting and metallic nanotubes.[15] In contrast, the $B_xC_yN_z$-SWNT network with nearly the same tube density and device geometry exhibited clear p-channel transistor behavior with on/off ratio as high as 10^5, indicating that the as-synthesized $B_xC_yN_z$-SWNTs were composed primarily of semiconducting nanotubes. These results are in line with our previous studies of CVD-grown $B_xC_yN_z$-SWNTs, verifying that B/N codoping is a realistic and promising way to produce purely semiconducting SWNTs and thereby to tackle the problem of electronic-type heterogeneity in pristine C-SWNTs.

To sum up, by exploiting the exfoliation and dispersion of C-SWNTs in imidazolium-based room-temperature ILs, we have innovatively improved the nanotube-substitution reaction methodology for achieving the high-efficiency synthesis of ternary $B_xC_yN_z$-SWNTs in bulk quantities. Combined TEM and EELS analyses together with XPS, FT-IR, and Raman spectroscopic studies confirmed the true substitutional incorporation of B and N dopants into the graphitic tube-shell lattice, with the single-layered nanotubular topology being well-preserved. As a consequence of B/N codoping, the electronic properties of the pristine C-SWNTs were successfully modified, and the thin-film electrical devices built from $B_xC_yN_z$-SWNTs exhibited good electrical performance characterized by semiconducting behavior. Finally, we remark that the present wet-chemistry-assisted substitution reaction strategy is not limited only to nanotubes; the capability of this approach potentially can also be extended to B/N codoping of graphene-related materials. Ongoing studies along this line are now underway.

■ ASSOCIATED CONTENT

Supporting Information. Experimental details; supplementary IR, Raman, and XPS characterization results; and the combined TEM and EELS results showing the deformation and collapse of the SWNTs at 1150 °C. This material is available free of charge via the Internet at http://pubs.acs.org.

■ AUTHOR INFORMATION

Corresponding Author
wwl@aphy.iphy.ac.cn; xdbai@aphy.iphy.ac.cn; egwang@pku.edu.cn

■ ACKNOWLEDGMENT

We are grateful for financial support from the NNSF (Grants 10874218, 50725209, and 20973195), MOST (Grants 2009DFA-01290 and 2007CB936203), and CAS (Grants KJCX2-YW-M13 and KJCX2-YW-W35) of China.

■ REFERENCES

(1) (a) Terrones, M.; Grobert, N.; Terrones, H. *Carbon* **2002**, *40*, 1665. (b) Ewels, C. P.; Glerup, M. *J. Nanosci. Nanotechnol.* **2005**, *9*, 1345. (c) Wang, W. L.; Bai, X. D.; Wang, E. G. *Int. J. Nanosci.* **2007**, *6*, 431. (d) Ayala, P.; Arenal, R.; Loiseau, A.; Rubio, A.; Pichler, T. *Rev. Mod. Phys.* **2010**, *82*, 1843.

(2) (a) Liu, A. Y.; Wentzovitch, R. M.; Cohen, M. L. *Phys. Rev. B* **1989**, *39*, 1760. (b) Saalfrank, P.; Rümler, W.; Hummel, H.-U.; Ladik, J. *Synth. Met.* **1992**, *52*, 1. (c) Miyamoto, Y.; Rubio, A.; Cohen, M. L.; Louie, S. G. *Phys. Rev. B* **1994**, *50*, 4976. (d) Yoshioka, T.; Suzuura, H.; Ando, T. *J. Phys. Soc. Jpn.* **2003**, *72*, 2656.

(3) (a) Wang, W. L.; Bai, X. D.; Liu, K. H.; Xu, Z.; Golberg, D.; Bando, Y.; Wang, E. G. *J. Am. Chem. Soc.* **2006**, *128*, 6530. (b) Xu, Z.; Lu, W. G.; Wang, W. L.; Gu, C. Z.; Liu, K. H.; Bai, X. D.; Wang, E. G.; Dai, H. J. *Adv. Mater.* **2008**, *20*, 3615.

(4) Enouz, S.; Stéphan, O.; Cochon, J.-L.; Colliex, C.; Loiseau, A. *Nano Lett.* **2007**, *7*, 1856.

(5) (a) Han, W. Q.; Bando, Y.; Kurashima, K.; Sato, T. *Appl. Phys. Lett.* **1998**, *73*, 3085. (b) Han, W. Q.; Bando, Y.; Kurashima, K.; Sato, T. *Chem. Phys. Lett.* **1999**, *299*, 368.

(6) (a) Golberg, D.; Bando, Y.; Kurashima, K.; Sato, T. *Chem. Phys. Lett.* **2000**, *323*, 185. (b) Golberg, D.; Bando, Y.; Kurashima, K.; Sato, T. *Diamond Relat. Mater.* **2001**, *10*, 63. (c) Bando, Y.; Golberg, D.; Mitome, M.; Kurashima, K.; Sato, T. *Chem. Phys. Lett.* **2001**, *346*, 29.

(7) (a) Terrones, M.; Golberg, D.; Grobert, N.; Seeger, T.; Reyes-Reyes, M.; Mayne, M.; Kamalakaran, R.; Dorozhkin, P.; Dong, Z. C.; Terrones, H.; Rühle, M.; Bando, Y. *Adv. Mater.* **2003**, *15*, 1899. (b) Han, W. Q.; Todd, P. J.; Strongin, M. *Appl. Phys. Lett.* **2006**, *89*, No. 173103. (c) Golberg, D.; Bando, Y.; Tang, C. C.; Zhi, C. Y. *Adv. Mater.* **2007**, *19*, 2413.

(8) (a) Golberg, D.; Bando, Y.; Han, W. Q.; Kurashima, K.; Sato, T. *Chem. Phys. Lett.* **1999**, *308*, 337. (b) Golberg, D.; Bando, Y.; Bourgeois, L.; Kurashima, K.; Sato, T. *Carbon* **2000**, *38*, 2017. (c) Borowiak-Palen, E.; Pichler, T.; Fuentes, G. G.; Graff, A.; Kalenczuk, R. J.; Knupfer, M.; Fink, J. *Chem. Phys. Lett.* **2003**, *378*, 516. (d) Borowiak-Palen, E.; Pichler, T.; Graff, A.; Kalenczuk, R. J.; Knupfer, M.; Fink, J. *Carbon* **2004**, *42*, 1123. (e) Liu, X. M.; Romero, H. E.; Gutierrez, H. R.; Adu, K.; Eklund, P. C. *Nano Lett.* **2008**, *8*, 2613.

(9) (a) Thess, A.; Lee, R.; Nikolaev, P.; Dai, H. J.; Petit, P.; Robert, J.; Xu, C. H.; Lee, Y. H.; Kim, S. G.; Rinzler, A. G.; Colbert, D. T.; Scuseria, G. E.; Tománek, D.; Fischer, J. E.; Smalley, R. E. *Science* **1996**, *273*, 483. (b) Girifalco, L. A.; Hodak, M.; Lee, R. S. *Phys. Rev. B* **2000**, *62*, 13104.

(10) (a) Fukushima, T.; Kosaka, A.; Ishimura, Y.; Yamamoto, T.; Takigawa, T.; Ishii, N.; Aida, T. *Science* **2003**, *300*, 2072. (b) Wang, J. Y.; Chu, H. B.; Li, Y. *ACS Nano* **2008**, *2*, 2540. (c) Sekitani, T.; Noguchi, Y.; Hata, K.; Fukushima, T.; Aida, T.; Someya, T. *Science* **2008**, *321*, 1468. (d) Mukai, K.; Asaka, K.; Sugino, T.; Kiyohara, K.; Takeuchi, I.; Terasawa, N.; Futaba, D. N.; Hata, K.; Fukushima, T.; Aida, T. *Adv. Mater.* **2009**, *21*, 1582.

(11) (a) Kim, S. Y.; Park, J.; Choi, H. C.; Ahn, J. P.; Hou, J. Q.; Kang, H. S. *J. Am. Chem. Soc.* **2007**, *129*, 1750. (b) Linss, V.; Rodilb, S.; Reinkec, P.; Garnierd, M.; Oelhafend, P.; Kreissige, U.; Richtera, F. *Thin Solid Films* **2004**, *467*, 76. (c) Mannan, M. A.; Nagano, M.; Kida, T.; Hirao, N.; Baba, Y. *J. Phys. Chem. Solids* **2009**, *70*, 20.

(12) (a) Komatsu, T. *J. Mater. Chem.* **2004**, *14*, 221. (b) Wada, Y.; Yap, Y. K.; Yoshimura, M.; Mori, Y.; Sasaki, T. *Diamond Relat. Mater.* **2000**, *9*, 620. (c) Caretti, I.; Jiménez, J.; Albella, J. M. *Diamond Relat. Mater.* **2003**, *12*, 1079. (d) Linss, V.; Hermann, I.; Schwarzer, N.; Kreissig, U.; Richter, F. *Surf. Coat. Technol.* **2003**, *163*, 220. (e) Kaufmann, J. H.; Metin, S.; Saperstein, D. D. *Phys. Rev. B* **1989**, *39*, 13053.

(13) (a) Kuhlmann, U.; Jantoljak, H.; Pfänder, N.; Bernier, P.; Journet, C.; Thomsen, C. *Chem. Phys. Lett.* **1998**, *294*, 237. (b) Sbai, K.; Rahmani, A.; Chadli, H.; Bantignies, J.-L.; Hermet, P.; Sauvajol, J.-L. *J. Phys. Chem. B* **2006**, *110*, 12388.

(14) (a) Maultzsch, J.; Reich, S.; Thomsen, C.; Webster, S; Czerw, R.; Carroll, D. L.; Vieira, S. M. C.; Birkett, P. R.; Rigo, C. A. *Appl. Phys. Lett.* **2002**, *81*, 2647. (b) Zhi, C. Y.; Bai, X. D.; Wang, E. G. *Appl. Phys. Lett.* **2002**, *80*, 3590.

(15) (a) Snow, E. S.; Novak, J. P.; Campbell, P. M.; Park, D. *Appl. Phys. Lett.* **2003**, *82*, 2145. (b) Hong, W.-K.; Lee, C.; Nepal, D.; Geckeler, K. E.; Shin, K.; Lee, T. *Nanotechnology* **2006**, *17*, 5675.